

**The following resources related to this article are available online at [www.sciencemag.org](http://www.sciencemag.org) (this information is current as of November 23, 2009 ):**

**Updated information and services**, including high-resolution figures, can be found in the online version of this article at:

<http://www.sciencemag.org/cgi/content/full/309/5731/140>

**Supporting Online Material** can be found at:

<http://www.sciencemag.org/cgi/content/full/1113346/DC1>

A list of selected additional articles on the Science Web sites **related to this article** can be found at:

<http://www.sciencemag.org/cgi/content/full/309/5731/140#related-content>

This article **cites 19 articles**, 14 of which can be accessed for free:

<http://www.sciencemag.org/cgi/content/full/309/5731/140#otherarticles>

This article has been **cited by** 37 article(s) on the ISI Web of Science.

This article has been **cited by** 22 articles hosted by HighWire Press; see:

<http://www.sciencemag.org/cgi/content/full/309/5731/140#otherarticles>

This article appears in the following **subject collections**:

Molecular Biology

[http://www.sciencemag.org/cgi/collection/molec\\_biol](http://www.sciencemag.org/cgi/collection/molec_biol)

Information about obtaining **reprints** of this article or about obtaining **permission to reproduce this article** in whole or in part can be found at:

<http://www.sciencemag.org/about/permissions.dtl>

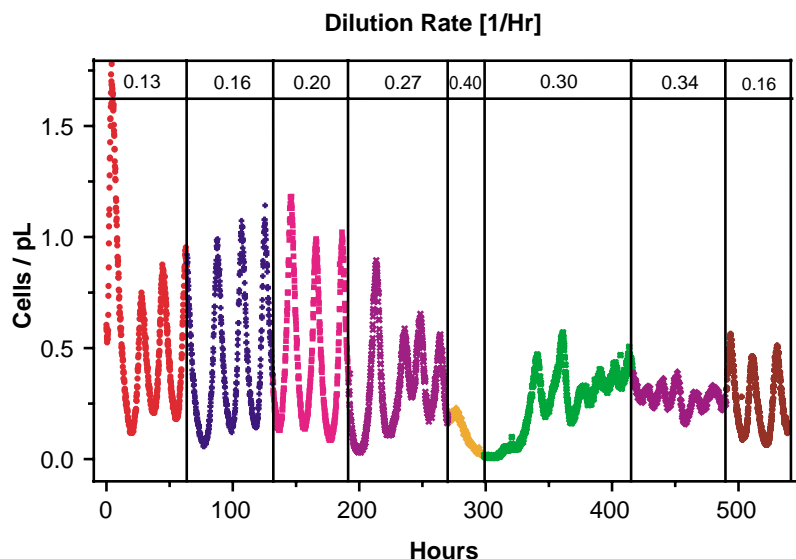


**Fig. 5.** Effects of the dilution rate on population dynamics of Top10F' cells with the population-control circuit ON. At high dilution rates (to 0.27, 0.30, and 0.34 hour<sup>-1</sup>), both the amplitude and the period of oscillations diminished. The culture was approaching wash-out at the highest dilution rate (0.40 hour<sup>-1</sup>). Large oscillations were recovered when a low dilution rate was restored toward the end of the experiment. Cells were grown at 32°C in LBK medium (14), buffered at pH 7.0.

mostat, in contrast, was routinely maintained for more than 200 hours and sometimes more than 500 hours (Fig. 5). In theory, the small population size in the microchemostat ( $\sim 10^2$  to  $\sim 10^4$  cells versus  $\sim 10^9$  cells in macroscale cultures) should reduce the overall rate at which mutants may occur and take over a population. Exactly how the cells lost regulation in the circuit-ON cultures (Fig. 3, culture 3, and Fig. 4, cultures 2, 3, 5, and 6) is unclear. A simple mutation rate versus population size argument would predict much longer lifetimes for maintaining circuit regulation.

We observed oscillations in cell density for both *E. coli* strains in the circuit-ON state. The MC4100Z1 strain had large-amplitude ( $\sim 2$  cells/pL) oscillations, which gradually decayed to a steady state (Fig. 3A). The Top10F' strain had smaller amplitude oscillations ( $\sim 1$  cell/pL) which continued for the length of the measurement (Figs. 4 and 5). Although the origin of these oscillations is unknown, they may be a consequence of the circuit interacting with the continuous culture mechanism of the microchemostat. It is also possible that the oscillations are entirely due to circuit regulation, as predicted by a simple mathematical model with biologically feasible parameters (14). These population-level oscillations are controllable—they only occur when the circuit is in the ON state—and they are more sustained and stable than those generated by synthetic oscillators operating in individual cells (17, 18).

An active approach to preventing biofilm formation in microfluidic devices enabled us to implement a miniaturized bioreactor that operates at a working volume of 16 nL, more than 300 times smaller than the smallest previous microfermentor (7). This miniaturized device

enabled automated culturing and monitoring of populations of  $\sim 100$  to  $\sim 10^4$  bacteria with instantaneous single-cell resolution. Reducing the reactor volume by a factor of  $10^5$  can, in theory, suppress the total mutation rate proportionately and hence prolong monitoring of genetically homogeneous populations (14). The microchemostat has enabled us to monitor the programmed behavior of bacterial populations for hundreds of hours despite strong selection pressure to evade population control, something that was not achieved in macroscopic reactors. Although we focused on the bacterial count and cell morphology, measurements can be readily extended to dynamic properties, for example, gene expression dynamics and distributions reported by fluorescence or luminescence. These capabilities enable long-term, low-cost, high-resolution

investigation of the phenotypical characteristics of many different cell strains, as well as natural and synthetic cellular networks under a matrix of conditions. This capability will greatly facilitate high-throughput screening applications in fields such as chemical genetics and pharmaceutical discovery.

#### References and Notes

1. J. Monod, *Ann. Inst. Pasteur (Paris)* **79**, 390 (1950).
2. A. Novick, L. Szilard, *Science* **112**, 715 (1950).
3. D. E. Dykhuizen, *Annu. Rev. Ecol. Syst.* **21**, 373 (1990).
4. M. S. Fox, *J. Gen. Physiol.* **39**, 267 (1955).
5. H. L. Smith, P. Waltman, in *The Theory of the Chemostat: Dynamics of Microbial Competition* (Univ. of Cambridge Press, Cambridge, ed. 1, 1995).
6. A. Novick, *Annu. Rev. Microbiol.* **9**, 97 (1955).
7. A. Zanzotto et al., *Biotechnol. Bioeng.* **87**, 243 (2004).
8. J. W. Kim, Y. H. Lee, *J. Korean Phys. Soc.* **33**, S462 (1998).
9. Y. Kostov, P. Harms, L. Randers-Eichhorn, G. Rao, *Biotechnol. Bioeng.* **72**, 346 (2001).
10. M. M. Maharbiz, W. J. Holtz, R. T. Howe, J. D. Keasling, *Biotechnol. Bioeng.* **85**, 376 (2004).
11. J. W. Costerton, Z. Lewandowski, D. E. Caldwell, D. R. Korber, H. M. Lappinocott, *Annu. Rev. Microbiol.* **49**, 711 (1995).
12. H. H. Topiwala, C. Hamer, *Biotechnol. Bioeng.* **13**, 919 (1971).
13. D. H. Larsen, R. L. Dimmick, *J. Bacteriol.* **88**, 1380 (1964).
14. Materials and methods are available as supporting material on Science Online.
15. L. You, R. S. Cox III, R. Weiss, F. H. Arnold, *Nature* **428**, 868 (2004).
16. M. B. Miller, B. L. Bassler, *Annu. Rev. Microbiol.* **55**, 165 (2001).
17. M. B. Elowitz, S. Leibler, *Nature* **403**, 335 (2000).
18. M. R. Atkinson, M. A. Savageau, J. T. Myers, A. J. Ninfa, *Cell* **113**, 597 (2003).
19. We thank M. Elowitz for MC4100Z1 cells, U. Alon for MG1655 cells, T. Ozdere for generating data for figs. S4 and S5, C. Collins for plasmid pLuxR, M. Barnett for technical assistance, and J. Leadbetter, C. Ward, T. Squires, J. Huang, and E. Kartalov for helpful discussions. Supported in part by the NSF and the Defense Advanced Research Projects Agency (contract no. N66001-02-1-8929).

#### Supporting Online Material

www.sciencemag.org/cgi/content/full/309/5731/137/DC1  
Materials and Methods  
Figs. S1 to S5  
Tables S1 and S2  
References and Notes

27 December 2004; accepted 10 May 2005  
10.1126/science.1109173

## tRNA Actively Shuttles Between the Nucleus and Cytosol in Yeast

Akira Takano,<sup>1</sup> Toshiya Endo,<sup>1,3,4</sup> Tohru Yoshihisa<sup>1,2\*</sup>

Previous evidence suggested that transfer RNAs (tRNAs) cross the nuclear envelope to the cytosol only once after maturing in the nucleus. We now present evidence for nuclear import of tRNAs in yeast. Several export mutants accumulate mature tRNAs in the nucleus even in the absence of transcription. Import requires energy but not the Ran cycle. These results indicate that tRNAs shuttle between the nucleus and cytosol.

Nuclear-encoded tRNAs are transcribed, processed in the nucleus, and exported to the cytosol to facilitate translation (1). Moreover, a nuclear pool of mature tRNAs also exists. In *Saccharomyces cerevisiae*, certain mutants defective in

nuclear transport and tRNA processing accumulate mature tRNAs in the nucleus, which suggests that nuclear mature tRNAs are intermediates waiting for tRNA export (2–5). Before export, aminoacyl-tRNA synthetases

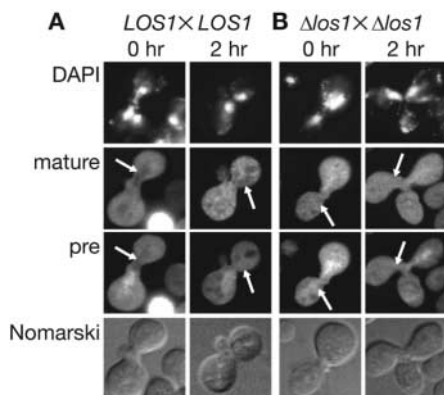


**Fig. 1.** Heterokaryon assay of nuclear import of tRNAs. (A) Heterokaryons formed from *MATα* cells with *sup3+* and *MATa* cells were incubated in yeast extract, peptone, and dextrose (YPD) for the indicated times and subjected to FISH using probes against mature *SptRNA-Met<sub>i</sub>* (mature) and pre-*SptRNA-Ser<sup>UGA</sup>* (pre). The nucleus and cell outlines are shown in the 4',6'-diamidino-2-phenylindole (DAPI) and Nomarski images, respectively. Target nuclei are marked by arrows. (B) Heterokaryon assays similar to (A) were performed with  $\Delta los1$  haploids.

may monitor their maturation (6). However, we recently found that tRNA-splicing endonuclease localizes to the mitochondrial surface in yeast and that an endonuclease mutant accumulates unspliced pre-tRNAs in the cytosol, which indicates that pre-tRNAs are exported to the cytosol and then spliced (7).

To understand the origin of nuclear mature tRNAs, we examined whether tRNAs are imported into the nucleus from the cytosol, using heterokaryon assays (8). In *S. cerevisiae*, a heterokaryon with two different nuclei sharing the same cytosol is formed from karyogamy-deficient *MATa* and *MATα* cells. To visualize tRNAs transcribed from one nucleus, a *sup3+* gene (*SptRNA-Ser<sup>UGA</sup>::SptRNA-Met<sub>i</sub>*) from *Schizosaccharomyces pombe* was introduced into the *MATα* strain. *sup3+* is transcribed and processed to mature *SptRNA-Ser<sup>UGA</sup>* and *SptRNA-Met<sub>i</sub>* in *S. cerevisiae* (9). Heterokaryons between the *MATa* cells (target) and the *MATα* cells with *sup3+* (donor) were subjected to fluorescence in situ hybridization (FISH). Pre-*SptRNA-Ser<sup>UGA</sup>* was detected in only one nucleus in a heterokaryon (Fig. 1A, pre, and fig. S2). In a wild-type background for tRNA export, mature *SptRNA-Met<sub>i</sub>* was excluded from target nuclei like endogenous tRNAs (Fig. 1A and fig. S4B).  $\Delta los1$  cells, lacking yeast exportin-t (10, 11), exhibit a

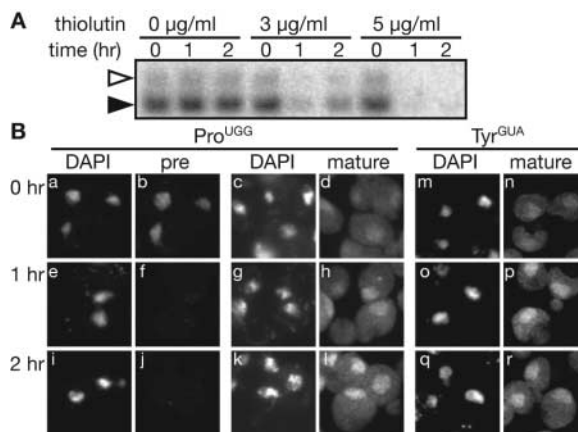


**Fig. 2.** Treatment with thiolutin causes accumulation of mature tRNA-*Pro<sup>UGG</sup>* in  $\Delta los1 \Delta msn5$  cells. (A)  $\Delta los1 \Delta msn5$  cells treated with the indicated concentrations of thiolutin were subjected to Northern hybridization with an anti-pre-tRNA-*Pro<sup>UGG</sup>* probe. White triangle, primary transcripts; black triangle, end-matured pre-tRNAs. (B) The cells treated with 5  $\mu\text{g/ml}$  thiolutin for the indicated times were subjected to FISH with probes against tRNA-*Pro<sup>UGG</sup>* and tRNA-*Tyr<sup>GUA</sup>*.

moderate defect in nuclear export of mature tRNAs (fig. S4B) (2). In  $\Delta los1$  heterokaryons, we observed more *SptRNA-Met<sub>i</sub>* in target nuclei (Fig. 1B). These data indicate that cytosolic mature tRNAs enter the nucleus.

Next, we investigated nuclear import of endogenous tRNAs in cells growing vegetatively. If all nuclear mature tRNAs are newly transcribed, transcription arrest should reduce the nuclear pool of tRNAs through their export. If mature tRNAs are supplied from the cytosol, this should not necessarily be true. A complicating factor is that the signal intensity of mature tRNAs in the wild-type nucleus is lower than that in the cytosol. To circumvent this problem, we used a  $\Delta los1 \Delta msn5$  double mutant. *Msn5p* is a homolog of mammalian exportin-5, which exports the tRNA-eEF1A complex and pre-miRNAs (microRNAs) (12–14).  $\Delta msn5$  by itself did not alter tRNA localization, but the  $\Delta los1 \Delta msn5$  mutant showed a strong synthetic defect in mature tRNA export (fig. S4), which suggests that *Msn5p* contributes to this export. Using this mutant, we analyzed the pool of nuclear tRNAs when transcription was blocked by thiolutin, an RNA polymerase inhibitor (15). In the presence of thiolutin, pre-tRNA-*Pro<sup>UGG</sup>* disappeared within 1 hour (Northern hybridization, Fig. 2A; FISH, Fig. 2B, pre), whereas mature tRNA-*Pro<sup>UGG</sup>* and tRNA-*Tyr<sup>GUA</sup>* accumulated in the nucleus (Fig. 2B, mature). Because no detectable transcription occurred under these conditions, nuclear mature tRNAs must have been supplied from the preexisting cytosolic pool.

To determine whether nuclear import of mature tRNAs requires energy,  $\Delta los1 \Delta msn5$  cells were incubated with  $\text{NaN}_3$  and 2-deoxyglucose (2-dG). Under these conditions, both the primary transcript of tRNA-*Pro<sup>UGG</sup>* and the gradient of mature tRNA-*Pro<sup>UGG</sup>* across the nuclear envelope (NE) were no longer detected (Fig. 3A and Fig. 3B, e). Reappearance of the primary transcript 10 min after  $\text{NaN}_3$  and 2-dG removal indicates rapid replenishment of intracellular adenosine triphosphate (Fig. 3A, -thiolutin). Nuclear

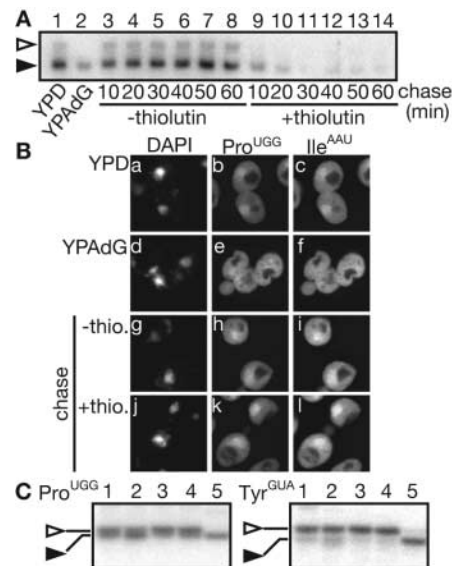


**Fig. 3.** Nuclear import of tRNAs is energy dependent. (A)  $\Delta los1 \Delta msn5$  cells grown in YPD (lane 1) were incubated with  $\text{NaN}_3$  and 2-dG (YPAdG) for 1 hour (lane 2). The cells were chased without (lanes 3 to 8) or with (lanes 9 to 14) thiolutin for the indicated times. Pre-tRNA-*Pro<sup>UGG</sup>* was detected by Northern hybridization. White triangle, primary transcripts; black triangle, end-matured pre-tRNAs. (B)  $\Delta los1 \Delta msn5$  cells were treated as in (A) and were harvested before the energy poison treatment (YPD), after the treatment (YPAdG), and after a 2-hour chase without (-thio.) or with (+thio.) thiolutin. Mature tRNA-*Pro<sup>UGG</sup>* and tRNA-*Ile<sup>AAU</sup>* were visualized with FISH. (C)  $\Delta los1 \Delta msn5$  cells grown in YPD (lane 1) were incubated in YPAdG (lane 2) and chased with thiolutin for 1 hour (lane 3) or 2 hours (lane 4). Aminoacylation states of tRNA-*Pro<sup>UGG</sup>* and tRNA-*Tyr<sup>GUA</sup>* were analyzed with acidic urea-PAGE. Lane 5 contains deacylated tRNA. White and black triangles represent aminoacylated and deacylated tRNAs, respectively.

accumulation of the mature tRNA was also reestablished after removal of  $\text{NaN}_3$  and 2-dG, even in the presence of thiolutin (Fig. 3B, h and k). We observed similar results with tRNA-*Ile<sup>AAU</sup>* encoded by intronless genes (Fig. 3B, i and l). These results indicate that

<sup>1</sup>Department of Chemistry, Graduate School of Science, <sup>2</sup>Research Center for Materials Science, <sup>3</sup>Institute for Advanced Research, <sup>4</sup>Core Research for Evolutionary Science and Technology, Japan Science and Technology Corporation, Nagoya University, Chikusa-ku, Nagoya 464-8602, Japan.

\*To whom all correspondence should be addressed. E-mail: tyoshihi@biochem.chem.nagoya-u.ac.jp

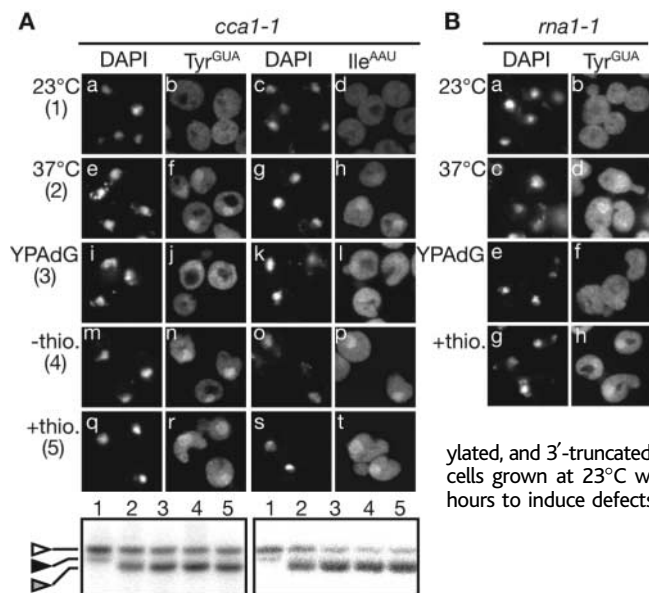


**Fig. 4.** Various tRNA species are imported into the nucleus, and import is Ran independent. **(A)** *cca1-1* cells grown at 23°C were incubated at 37°C for 3 hours, treated with NaN<sub>3</sub> and 2-dG for 3 hours at 37°C (YPAdG), and then chased without (–thio.) or with (+thio.) thiolutin for 1.5 hours. Samples were analyzed using FISH (top) and Northern hybridization (bottom) with indicated probes. White, black, and gray triangles represent aminoacylated, deacylated, and 3'-truncated tRNAs, respectively. **(B)** *rna1-1* cells grown at 23°C were incubated at 37°C for 1.5 hours to induce defects and then processed as in (A).

**References and Notes**

1. A. K. Hopper, E. M. Phizicky, *Genes Dev.* **17**, 162 (2003).
2. S. Sarkar, A. K. Hopper, *Mol. Biol. Cell* **9**, 3041 (1998).
3. H. Grosshans, E. Hurt, G. Simos, *Genes Dev.* **14**, 830 (2000).
4. W. Feng, A. K. Hopper, *Proc. Natl. Acad. Sci. U.S.A.* **99**, 5412 (2002).
5. S. Sarkar, A. K. Azad, A. K. Hopper, *Proc. Natl. Acad. Sci. U.S.A.* **96**, 14366 (1999).
6. E. Lund, J. E. Dahlberg, *Science* **282**, 2082 (1998).
7. T. Yoshihisa, K. Yunoki-Esaki, C. Ohshima, N. Tanaka, T. Endo, *Mol. Biol. Cell* **14**, 3266 (2003).
8. R. Azpiroz, R. A. Butow, *Mol. Biol. Cell* **4**, 21 (1993).
9. I. Willis et al., *EMBO J.* **3**, 1573 (1984).
10. K. Hellmuth et al., *Mol. Cell. Biol.* **18**, 6374 (1998).
11. G.-J. Arts, S. Kuersten, P. Romby, B. Ehresmann, I. W. Mattaj, *EMBO J.* **17**, 7430 (1998).
12. A. Kaffman, N. M. Rank, E. M. O'Neill, L. S. Huang, E. K. O'Shea, *Nature* **396**, 482 (1998).
13. M. T. Bohnsack et al., *EMBO J.* **21**, 6205 (2002).
14. E. Lund, S. Güttinger, A. Calado, J. E. Dahlberg, U. Kutay, *Science* **303**, 95 (2004).
15. T. Kadowaki et al., *J. Cell Biol.* **126**, 649 (1994).
16. C. L. Wolfe, A. K. Hopper, N. C. Martin, *J. Biol. Chem.* **271**, 4679 (1996).
17. D. Görlich, U. Kutay, *Annu. Rev. Cell Dev. Biol.* **15**, 607 (1999).
18. S. Kadaba et al., *Genes Dev.* **18**, 1227 (2004).
19. F. J. Iborra, D. A. Jackson, P. R. Cook, *Science* **293**, 1139 (2001).
20. We thank A. K. Hopper, K. Weis, P. A. Silver, Y. Ohya, and J. L. Brodsky for experimental materials and critical reading of our manuscript. We appreciate support from our lab members, especially T. Makio and S. Nishikawa. This work was supported by grants-in-aid for Scientific Research from the Ministry of Education, Culture, Sports, Science, and Technology of Japan.

**Supporting Online Material**

www.sciencemag.org/cgi/content/full/1113346/DC1  
 Materials and Methods  
 SOM Text  
 Figs. S1 to S6  
 Tables S1 to S3  
 References

8 April 2005; accepted 9 May 2005  
 Published online 19 May 2005;  
 10.1126/science.1113346

Include this information when citing this paper.

the import of both intron-containing and intronless tRNAs requires energy.

We analyzed aminoacylation states of mature tRNAs imported into the nucleus using acidic urea–polyacrylamide gel electrophoresis (urea-PAGE). Mature tRNA-Pro<sup>UGG</sup> and tRNA-Tyr<sup>GUA</sup> in *Δlos1 Δmsn5* cells were present primarily as slower migrating forms even after the chase with thiolutin (Fig. 3C, lanes 1, 3, and 4). These forms were converted to faster migrating forms by base treatment (lane 5), which indicates that the slower migrating tRNAs are aminoacylated. Therefore, imported tRNAs exist mainly in aminoacylated forms in the nucleus.

We asked whether 3'-truncated tRNAs are imported. *cca1-1* cells are deficient in both de novo formation and repair of 3'-terminal CCA ends of tRNAs (16), and also in tRNA export (4). We therefore treated *cca1-1* cells with NaN<sub>3</sub> and 2-dG at a restrictive temperature to abolish the mature tRNA gradient across the NE and chased them with thiolutin. tRNA-Tyr<sup>GUA</sup> and tRNA-Ile<sup>AAU</sup> reaccumulated in the nucleus to similar levels (Fig. 4A, q to t), although the proportions of the 3'-truncated forms of these tRNAs were different (Fig. 4A, bottom). Taken together with the fact that tRNAs in *Δlos1 Δmsn5* cells were full-length tRNAs, these results indicate that various forms of tRNAs are imported.

To determine the contribution of Ran guanosine triphosphatase (GTPase) (17), we examined tRNA import in *rna1-1* cells defective in RanGAP (Ran GTPase activating protein). The *rna1-1* cells accumulated mature tRNA-Tyr<sup>GUA</sup> in the nucleus at 37°C (2), and this tRNA gradient disappeared upon treatment with NaN<sub>3</sub> and 2-dG (Fig. 4B, 37°C, YPADG). When the cells were transferred to medium with thiolutin, mature tRNA-Tyr<sup>GUA</sup> was reaccumulated (Fig. 4B, +thio.). Because

protein import ceased at 37°C in *rna1-1* cells (fig. S5), these results suggest that tRNA import is Ran independent.

Our results indicate that nuclear mature tRNAs are supplied from the cytosol and that tRNAs shuttle between these two compartments. Shuttling may contribute to tRNA quality control, because tRNAs have long lifetimes and may run the risk of inappropriate modifications (18). A quality-control system in the nucleus may repair or filter out inactive tRNAs from those shuttling through the nucleus and provide only active tRNAs back to the cytosol. Another controversial possibility would be to supply tRNAs for nuclear translation (19).

## Variable Control of Ets-1 DNA Binding by Multiple Phosphates in an Unstructured Region

Miles A. Pufall,<sup>1</sup> Gregory M. Lee,<sup>2</sup> Mary L. Nelson,<sup>1</sup> Hyun-Seo Kang,<sup>2</sup> Algirdas Velyvis,<sup>3</sup> Lewis E. Kay,<sup>3</sup> Lawrence P. McIntosh,<sup>2</sup> Barbara J. Graves<sup>1\*</sup>

Cell signaling that culminates in posttranslational modifications directs protein activity. Here we report how multiple Ca<sup>2+</sup>-dependent phosphorylation sites within the transcription activator Ets-1 act additively to produce graded DNA binding affinity. Nuclear magnetic resonance spectroscopic analyses show that phosphorylation shifts Ets-1 from a dynamic conformation poised to bind DNA to a well-folded inhibited state. These phosphates lie in an unstructured flexible region that functions as the allosteric effector of auto-inhibition. Variable phosphorylation thus serves as a "rheostat" for cell signaling to fine-tune transcription at the level of DNA binding.

Proteins are activated or repressed by post-translational modifications in response to extracellular cues. Phosphorylation, a typical modification, often accumulates at multiple sites until a threshold level is reached. The

outcome is described as a sharp on/off switch of protein activity (1, 2). However, biological processes may need more sensitive regulation. Despite this need, variable regulation of protein activity in response to multiple modifica-